Physica E 145 (2023) 115496

Contents lists available at ScienceDirect

Physica E: Low-dimensional Systems and Nanostructures

journal homepage: www.elsevier.com/locate/physe

Quantum Floquet spectra of surface and bulk state of topological insulator

Upendra Kumar [a], Vipin Kumar [b], Ajay Kumar Kushwaha [c], Sung Beom Cho [d,*]

[a] Virtual Engineering Center, Technology Convergence Division, Korea Institute of Ceramic Engineering and Technology (KICET), Jinju 52851, South Korea
[b] Department of Physics, Yeungnam University, Gyeongsan, Gyeongbuk 38541, South Korea
[c] Department of Metallurgy Engineering and Materials Science, Indian Institute of Technology Indore, Khandwa Road, Simrol, Indore 453552, India
[d] Department of Materials Science and Engineering, Ajou University, Suwon 16499, South Korea

ARTICLE INFO

Keywords:
Topological insulators
Floquet theory
Collapse revival spectra
Bloch–Siegert shift
Rabi frequency

ABSTRACT

Topological insulators are a new class of material, which consists of insulating bulk and conducting surface state. In this study, we investigated the behavior of bulk and surface state of topological insulator under a high frequency electromagnetic field, produce a kind of oscillation called as Floquet oscillation. We successfully identified the classical and quantum behavior of Floquet oscillation in the prospective of collapse revival spectra. This work shows the bulk and surface states behavior of a topological insulator with the help of Floquet and Rabi frequency and describes the dominancy of Floquet oscillation in the low energy physics. Numerical simulation has been applied for verifying the Floquet approximation.

1. Introduction

There is a specific type of material, which has an insulator bulk (trivial state) but has conducting states on the surface, allowing electrons to only travel along the surface (non-trivial state), known as topological insulators (TI) [1]. Ordinary insulators may have conductive surface states [2], but TI surface states are topologically protected by the time-reversal symmetry. These surface states are also protected from non-magnetic disorders. It is described in recent research that surface-bulk correspondence can be obtained even when the bulk is gapless by virtue of point touchings of non-degenerate conduction and valence bands [3]. Eventually, it can be said that a bulk spectral gap is an important ingredient in any topological phase.

In condensed matter physics, the electronic parameters of some structures can be controlled by the high-frequency electromagnetic field. Such mechanism is known as Floquet engineering, which has mathematical formulation known as Floquet theory [4] for periodically driven quantum systems and produces many fundamental effects [5]. For the study of the off-resonance case, there is an application of Floquet approximation in the place of rotating wave approximation in Dirac fermionic systems [6]. By using Floquet engineering, the electronic bandgap of graphene has been generated [7]. Floquet engineering has also shown its importance in the generation of Floquet Weyl semimetal state via off-resonant light [8]. By application of Floquet theory, the nuclear magnetic resonance (NMR) spinning sidebands for homonuclear two-spin systems have been described [9]. The Floquet–Magnus expansion is used as an alternative expansion scheme for solving the time-dependent linear differential equation: a central problem in solid-state NMR [10]. The application of photon has already been described for probing topological edge or surface states [11]. The Floquet operators of periodically driven systems can be divided into topologically distinct (homotopy) classes [12]. Topological insulator surface Dirac fermions hybridize with an intense ultrashort midinfrared pulse whose energy is below the bulk bandgap to form Floquet–Bloch bands, as confirmed by time and angle resolved photoemission spectroscopy [13]. It is possible to study the transition between Floquet–Bloch states and Volkov states on the surface of the topological insulator, Bi_2Se_3, by using time and angle resolved photoemission spectroscopy [14]. Using linear and circular polarizations, it is possible to characterize the electron spectral function of the topological surface excitations [15]. Floquet boundary states with spin-polarized currents emerge as a result of a topological transition between the illuminated regions [16].

The Floquet band structure can be altered by the application of time-periodic perturbations [17]. In a semiconductor quantum well (trivial phase), a topological state can be induced with the help of Floquet theory [18]. The quantum information can be encoded by Floquet Majorana fermions if there is no break in the fermion parity conservation by the driving potential [19]. There is a design of guided-wave photonic bandgap devices with the help of Bloch–Floquet theory [20]. By using Floquet theory in Cooper pair pumping, it has been shown that the derivative of the Floquet quasi-energy with respect to the superconducting phase difference is proportional to the total charge transmitted through the circuit [21]. Floquet topological states have

* Corresponding author at: Department of Materials Science and Engineering, Ajou University, Suwon 16499, South Korea.
E-mail address: csb@ajou.ac.kr (S.B. Cho).

https://doi.org/10.1016/j.physe.2022.115496
Received 28 March 2022; Received in revised form 28 July 2022; Accepted 15 September 2022
Available online 20 September 2022

also been applied in the ultrafast spintronics, and strongly correlated electron systems [22]. Therefore, Floquet theory plays an important role in many areas of physics.

There are some challenges that may be interesting for the future developments of Floquet engineering. For example, we need to replace the laser with a more effective field generator to create Floquet-engineered devices that fit our pockets. The application of metamaterials and near-field optics will be a significant step forward in this area [22]. It is exciting to explore Floquet state functions that are not available in static systems. Using correlated electrons [23,24] and even single spins, devices with nontrivial output signals due to the dynamics of the Floquet state have been suggested [25]. To explore strongly correlated systems such as fractional quantum Hall states or even dynamical gauge fields in the future, it will be necessary to inhibit heating in Floquet systems [26].

The periodic exchange of energy between the electromagnetic field and two-level system is known as Rabi oscillations [27]. Rabi oscillations and Floquet states have similar behavior i.e. both are related with a periodically time-varying Hamiltonian [6]. In other words, Rabi oscillation is a close cousin of Floquet oscillation in the resonance case. In the theoretical modeling of Rabi oscillations, the externally applied field has been decomposed into two mutually counter-rotating fields. In the case of resonance and weak-driving field limit, the co-rotating component has a tendency to interact with spins (constructively) and leads to a Rabi frequency that scales linearly with the driving strength [28]. The rotating-wave approximation has been applied for driving the expression of Rabi frequency [29]. When the driving field is very strong, the Rabi frequency approaches towards the Larmor frequency and the counter-rotating term produces a shift in the level transition, called as Bloch–Siegert shift [30].

During the time evolution, if the wave function occurs a periodic recurrence from its original, produces a phenomenon, known as collapse–revival [31]. In the beginning, the existence of collapse and revival phenomenon was found in the Talbot effect [32], where optical signal amplitude collapses and revives automatically. Such phenomenon has also been studied in slightly anharmonic oscillator by using analytical and numerical approaches [33]. In the wave packets of Rydberg atoms, collapse–revival, fractional revivals and super revival structures were seen [34]. The Jaynes–Cummings model has been applied for theoretical modeling of collapse–revival phenomena [35]. In this work, the collapse–revival phenomenon has been studied from the perspective of Floquet oscillation by using the Jaynes–Cummings model.

Generally, the light-matter interaction has been treated in the semi-classical way in the Floquet theory [36,37] but here we have considered light-matter interaction in purely quantum form by mapping TI Hamiltonian into the Jaynes–Cummings model [38]. In this article, it is shown how we can distinguish the surface and bulk state of TI by application of quantum Floquet oscillation, which is a very difficult task in classical treatment. The Rabi oscillation is also studied in point of the quantum electromagnetic field. The role of the Bloch–Siegert shift has been shown in the Rabi oscillation. The comparison between Floquet and Rabi oscillation is performed; both have different natures in the surface and bulk of TI. Finally, numerical simulation justifies the analytical expression of Floquet frequency.

2. Floquet collapse–revival spectra

At first, it appeared that an external magnetic field was required to achieve quantum Hall effect (QHE); however, Haldane claimed that QHE can still be detected even in the absence of an external magnetic flux [39]. He broke time reversal symmetry (TRS) by introducing direction-dependent complex next-nearest-neighbor hopping in a honeycomb lattice, such as graphene. The only necessary criterion to witness QHE is the presence of this broken TRS. These quantized (integer) values of the Chern number provide a plateau in the Hall conductivity when the Fermi energy lies in the bulk gap. The model that was proposed by Haldane is a two-band system, with the bands being described by a topological invariant known as the Chern number. In quantum many-body systems, investigation of the topological features associated with the Haldane model has advanced quickly [40]. There is a specific type of TI with broken time-reversal symmetry, known as the Chern insulator. With help of tight-binding approximation, the low-energy Hamiltonian [41] of such TI derived as:

$$H_0 = \upsilon p_x \sigma_x + \upsilon p_y \sigma_y + \left[C - B(p_x^2 + p_y^2)\right]\sigma_z. \tag{1}$$

The $\sigma_{x,y,z}$ are Pauli matrices (real electronic spin), $C = m\upsilon^2$ is the bandgap, υ is speed of electron, m and B^{-1} have dimensions of mass. The Z_2 index for the topologically trivial state is always zero, so the Dirac equation becomes topologically trivial. After modification in the mass term $C \to C - Bp^2$, Z_2 index becomes 1 (non-trivial state → metallic surface) for $BC > 0$ and 0 (trivial state → insulator bulk) for $BC < 0$. If we fix B, the topological quantum phase transition can be shown from a topologically trivial system to a nontrivial system by changing the sign of mass term C. A detailed description of the topological insulator phase has been given in the article of S.Q. Shen [41]. In presence of vector potential (interaction with electromagnetic radiation), the above Hamiltonian [Eq. (1)] can be written as (detail in the supplementary information section(I)):

$$\begin{aligned} H = &\left[c_A^\dagger \upsilon(p_x - ip_y)c_B + e^{-i\omega t}c_A^\dagger \lambda b c_B + c.c.\right] \\ &+ \left[C - B\left(p_x^2 + p_y^2\right)\right]\left(c_A^\dagger c_A - c_B^\dagger c_B\right) \\ &- \left[B\left(p_x\frac{\lambda b}{\upsilon} + ip_y\frac{\lambda b}{\upsilon}\right)e^{-i\omega t} + c.c.\right]\left(c_A^\dagger c_A - c_B^\dagger c_B\right). \end{aligned} \tag{2}$$

The vector potential has form $A(t) = \mathrm{Re}(A_0 e^{i\omega t})$, where A_0 is the amplitude of the vector potential, $c.c.$ is for the complex conjugate, and ω is external driving frequency. The vector potential has circularly polarized form i.e. $A_{x0} = A(t)$, $A_{y0} = A(t)e^{i\beta}$, and the angle of polarization of the incident light is $\beta = \frac{r\pi}{2}$ ($r = \pm 1, \pm 3, ..$). The relation between vector potential and coupling constant (λ and λ^*) is $\frac{eA_{x0}}{c}\upsilon = \lambda b$ and $-\frac{eA_{x0}^*}{c}\upsilon = \lambda^* b^\dagger$. The b and $b^\dagger$ are creation and annihilation operators for the photons, while $c^\dagger(c)$ is creation (annihilation) operator in spin up or down state of electron, A or B representing spin up or down state of electron.

The Hamiltonian H [Eq. (2)] can be transformed into the Jaynes–Cummings model by using unitary transformation (detail in the supplementary information section(II)). For making the mathematical model simple, it is considered that only one electron is present in whole process with a spin-up or spin-down state. Therefore, each state has either presence of no electron and no hole or one electron and one hole. The non-zero probability amplitudes have form $\phi_{01}^{n+1}(t)$ and $\phi_{10}^{n+1}(t)$, where, n belongs to the number of photons, 1 belongs to the electron and 0 belongs to the hole. Due to presence of huge number of photon in the whole process, it can be considered that $n \approx n+1$. By using the evolution equation $i\hbar(\partial|\phi(t)\rangle/\partial t) = H|\phi(t)\rangle$, the equation of probability amplitudes can be written as ($\hbar = 1$, $p_x = p\cos\theta$ and $p_y = p\sin\theta$, detail in the supplementary information section(IV)):

$$\begin{aligned} i\frac{\partial}{\partial t}\begin{bmatrix}\phi_{01}^{n+1}(t)\\ \phi_{10}^{n+1}(t)\end{bmatrix} &= \begin{bmatrix}-\left(C - Bp^2\right) & p\upsilon e^{i\theta}\\ p\upsilon e^{-i\theta} & \left(C - Bp^2\right)\end{bmatrix}\begin{bmatrix}\phi_{01}^{n+1}(t)\\ \phi_{10}^{n+1}(t)\end{bmatrix} \\ &+\lambda\sqrt{n+1}\left(\begin{bmatrix}0 & 0\\ 1 & 0\end{bmatrix} + \frac{Bpe^{i\theta}}{\upsilon}\begin{bmatrix}1 & 0\\ 0 & -1\end{bmatrix}\right)\begin{bmatrix}\phi_{01}^{n+1}(t)\\ \phi_{10}^{n+1}(t)\end{bmatrix}e^{-i\omega t} \\ &+\lambda^*\sqrt{n+1}\left(\begin{bmatrix}0 & 1\\ 0 & 0\end{bmatrix} + \frac{Bpe^{-i\theta}}{\upsilon}\begin{bmatrix}1 & 0\\ 0 & -1\end{bmatrix}\right)\begin{bmatrix}\phi_{01}^{n+1}(t)\\ \phi_{10}^{n+1}(t)\end{bmatrix}e^{i\omega t}. \end{aligned} \tag{3}$$

The numerical simulation has been performed for solving above Eq. (3) with the help of *Mathematica Software* [42]. The equation of probability amplitude [Eq. (3)] has been solved by using *NDSolve* routine. The results found via numerical simulation are mentioned in

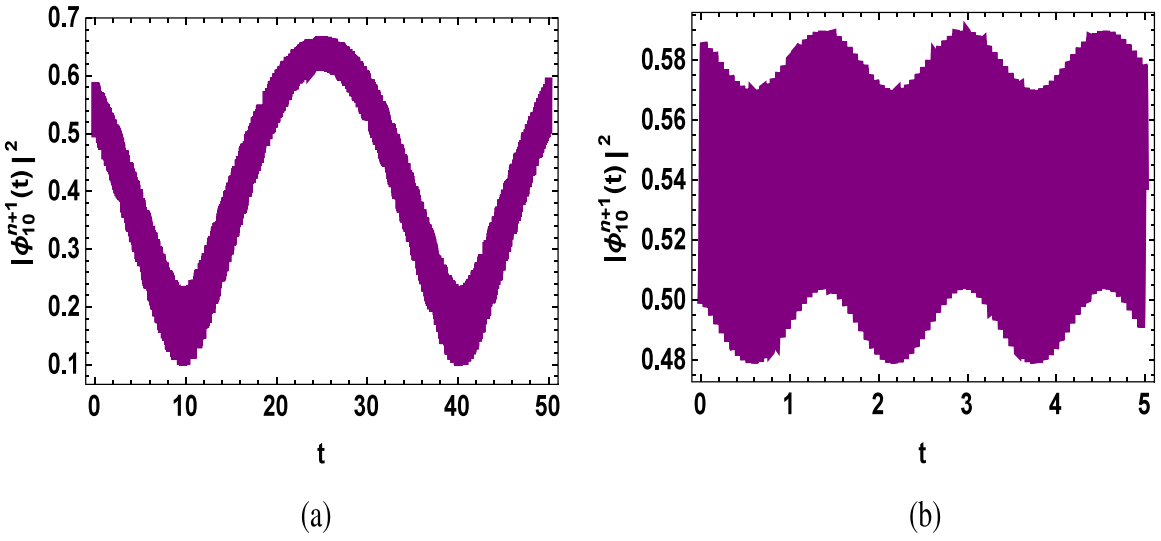

Fig. 1. The plot of probability amplitude with the Floquet frequency belongs to numerical simulation ($T_{\text{Floq-Simulation}}$) **(a)** with a period of 31.28 **(b)** with a period of 1.60. Parameters detailed are given in the Table 1 caption.

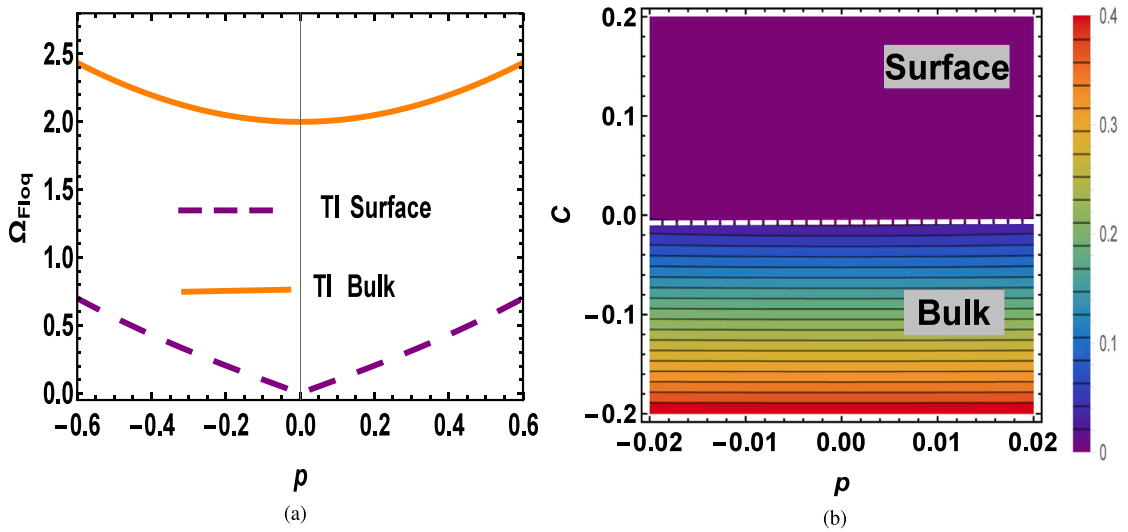

Fig. 2. **(a)** The plot between Floquet frequency Ω_{Floq} vs p ($C = 1$) and **(b)** contour plot of Floquet frequency by using Eqs. (7) and (8). For plotting, we have taken $v = 1$, $B = 1$ and $\omega = 1$. Parameters are considered in the unit of ω^{-1}. The surface belongs to the $C > 0$ and bulk belongs to the $C < 0$.

the Table 1. The time period of the probability amplitude is shown in Fig. 1.

The Floquet engineering is applied in far from resonance case and the external driving frequency ω has too higher value than conventional Rabi frequency and the carrier excitation energy. For solving the evolution equation ($H\psi = i\hbar\partial\psi/\partial t$), the wavefunction ψ has been expanded in the series of harmonics i.e. $\psi = \psi_s + e^{-i\omega t}\,\psi_p + e^{i\omega t}\,\psi_m + \cdots$.. with consideration that the coefficients ψ_s, ψ_p and ψ_m varies very slowly in perspective of the external driving frequency ω. Therefore, the terms of the order of $1/\omega^2$ have been neglected and final evolution equation becomes $i\hbar(\partial\psi_s/\partial t) = H_{\text{EFF}}\,\psi_s$, where

$$H_{\text{EFF}} \equiv \left(H_0 + \frac{1}{\omega}\left[H_m,\ H_p\right]\right). \tag{4}$$

The eigenvalues (positive) related with H_{EFF} are known as the Floquet frequency of the wave function (detail in the supplementary information section(III)). Now, comparing above Eq. (3) with $H = H_0 + e^{-i\omega t}\,H_p + e^{i\omega t}\,H_m$ and applying Floquet approximation, the expression of H_0, H_p and H_m can be found. By inserting these expressions in Eq. (4), the expression of H_{EFF} has form:

$$H_{\text{EFF}} = \begin{bmatrix} \left(Bp^2 - C + \frac{(n+1)|\lambda|^2}{\omega}\right) & \frac{e^{i\theta}pv\left(\omega - \frac{2B(n+1)|\lambda|^2}{v^2}\right)}{\omega} \\ \frac{e^{-i\theta}pv\left(\omega - \frac{2B(n+1)|\lambda|^2}{v^2}\right)}{\omega} & -\left(Bp^2 - C + \frac{(n+1)|\lambda|^2}{\omega}\right) \end{bmatrix}. \tag{5a}$$

Where:

$$H_p = \lambda\sqrt{n+1}\left(\begin{bmatrix} 0 & 0 \\ 1 & 0 \end{bmatrix} + \frac{Be^{i\theta}p}{v}\begin{bmatrix} 1 & 0 \\ 0 & -1 \end{bmatrix}\right), \tag{5b}$$

$$H_m = \lambda^*\sqrt{n+1}\left(\begin{bmatrix} 0 & 1 \\ 0 & 0 \end{bmatrix} + \frac{Be^{i\theta}p}{v}\begin{bmatrix} 1 & 0 \\ 0 & -1 \end{bmatrix}\right). \tag{5c}$$

Table 1
T belongs to the time period Floquet oscillations in TI. The time periods in this table are measured by considering $\lambda = 1$, $n = 99$, $\hbar = 1$, $\omega = 100$, $B = 1$, $C = \pm 1$ (surface/bulk), $\theta = \frac{\pi}{4}$ and $v = 1$. Parameters are considered in the units of λ^{-1}.

TI surface					
p	0. 1	0.2	0.3	0. 4	0.5
T_{Floq} simulation	31.28	15.43	10.05	7.32	5.65
T_{Floq} derivation	31.26	15.40	10.03	7.29	5.62
TI bulk					
p	0. 1	0.2	0.3	0. 4	0.5
T_{Floq} simulation	1.60	1.55	1.51	1.45	1.40
T_{Floq} derivation	1.56	1.53	1.49	1.43	1.36

Here, $|\lambda|^2 = \lambda\lambda^*$. The eigenvalue of H_{EFF} [Eq. (5a)] gives following Floquet frequency with quantized nature

$$\Omega_{Floq} = \left[p^2v^2 + \left(C - Bp^2\right)^2 - \frac{2(n+1)|\lambda|^2(C+Bp^2)}{\omega} + \frac{|\lambda|^4(n+1)^2\left(4B^2p^2+v^2\right)}{\omega^2v^2} \right]^{\frac{1}{2}}. \tag{6}$$

By choosing a specific value $|\lambda|^2(n+1) = \omega|C|$, the behavior of Floquet frequency (Ω_{Floq}) is able to distinguish the surface and bulk state of TI at the Dirac point. The number of photons n and external field ω are experimentally controlled parameters. Therefore, the above expression [Eq. (6)] of Floquet frequency becomes:
First Case : If B is positive and C is negative i.e. $BC < 0$ i.e. TI bulk state:

$$\Omega_{Floq-Bulk} = \sqrt{\frac{\left(B^2p^2+v^2\right)\left(4C^2+p^2v^2\right)}{v^2}}. \tag{7}$$

Second Case : If B and C are positive i.e. $BC > 0$ i.e. TI surface state:

$$\Omega_{Floq-Surface} = p\sqrt{B^2\left(\frac{4C^2}{v^2}+p^2\right) - 4BC + v^2}. \tag{8}$$

It is clearly depicted in Fig. 2, at Dirac point ($p = 0$), the minimum value of Floquet frequency is zero for the surface state of TI (gapless modes). On the other hand in case of bulk of TI, the Floquet frequency has a non-zero value (gapped). Therefore, the topological surface and bulk state can be distinguished with help of the Floquet oscillation. The analytical expressions of the Floquet frequency [Eqs. (7) and (8)] are completely agreeing with the numerical simulation. The comparison between numerical and analytical results is shown in the Table 1.

The Bloch equations derived for TI in prospective of Floquet theory i.e. $i\hbar(\partial|\phi(t)\rangle/\partial t) = H_{EFF}|\phi(t)\rangle$, have form ($\hbar = 1$):

$$i\frac{\partial\phi_{01}^{n+1}(t)}{\partial t} = e^{i\theta}p\left[v - \frac{2B(n+1)|\lambda|^2}{v\omega}\right]\phi_{10}^{n+1}(t) + \left[Bp^2 - C + \frac{(n+1)|\lambda|^2}{\omega}\right]\phi_{01}^{n+1}(t); \tag{9a}$$

$$i\frac{\partial\phi_{10}^{n+1}(t)}{\partial t} = e^{-i\theta}p\left[v - \frac{2B(n+1)|\lambda|^2}{v\omega}\right]\phi_{01}^{n+1}(t) - \left[Bp^2 - C + \frac{(n+1)|\lambda|^2}{\omega}\right]\phi_{10}^{n+1}(t). \tag{9b}$$

Assume that the initial state of the system was $|\phi(0)\rangle = |0,\zeta\rangle$ and the atom is situated in the ground state $|0\rangle$. The external field is present in the coherent state $|\zeta\rangle$. Therefore, the initial values of the probability amplitudes are $\phi_{01}^{n+1}(t) = \langle n+1|\zeta\rangle$ and $\phi_{10}^{n+1}(t) = 0$, which gives:

$$|\phi_{01}^{n+1}(t)|^2 = \frac{|\zeta|^{2n}}{n!}e^{-|\zeta|^2}.$$

Where ζ is a complex number, $\bar{n}(= |\zeta|^2)$ belongs to the average number of photon in the initial coherent state. Therefore, the probability of state $\phi_{01}^{n+1}(t)$ is

$$P_1(t) = \sum_n \frac{(\bar{n})^n}{n!}e^{-\bar{n}}\left[\frac{p^2v^2\left(\omega - \frac{2B|\lambda|^2(n+1)}{v^2}\right)^2}{\omega^2\Omega_{Floq}^2}\right]\sin^2\left(\Omega_{Floq}t\right). \tag{10}$$

By plotting $P_1(t)$, the nature of collapse–revival spectra can be seen, shown in Fig. 3**(a)**. According to semiclassical theory, the atom in the excited state cannot make transition to the lower level in the absence of a driving field. The transition from the higher level to the lower level in the vacuum is allowed in the completely quantum mechanical treatment owing to the spontaneous emission. Spontaneous emission can be seen in Eq. (10), where the spontaneously released photon contributes to the single mode of the field. Spontaneous emission is responsible for the collapse–revival phenomena that can be physically explained with the help of Eq. (10). For a particular value of n, every term of summation of Eq. (10) belongs to the Floquet oscillation. The relative weight of every value of n can be determined with the help of photon distribution function $((\bar{n})^n/n!)e^{-\bar{n}}$. In beginning i.e. $t = 0$, the atoms are present at definite state, so all the term of summation [Eq. (10)] are correlated. As time passes, the Floquet oscillation related with different excitations have different frequencies, start to uncorrelated leads to a collapse. After some time, the correlation is restored and revival comes into the picture. This pattern repeats itself, resulting in an unlimited number of revivals, depicted in Fig. 3**(a)**. *The essential thing worth noting is that revivals only happen due to the quantization of the number of photons.* Thus, it can be said, revival is a genuine quantum phenomenon. If we consider a continuous photon distribution (without zeros), the collapse will come into the picture like the classical random field, but no revivals. The conventional Rabi frequency ω_R is equivalent to $\sqrt{n+1}\,\lambda$ [43] i.e. we replace $\sqrt{n+1}\,\lambda = \omega_R$ in Eq. (10), classical behavior of Floquet frequency comes in to the picture. In the case of classical behavior of Floquet frequency, sinusoidal behavior can be seen, depicted in Fig. 3**(b)**. Because of too much overlapping between surface and bulk Floquet oscillation [Fig. 3**(b)**], it is quite difficult to distinguish surface and bulk by classical treatment of Floquet oscillation.

It is clearly depicted in Fig. 3**(a)**, the collapse of Floquet frequency happens and revival of it performs after some time. There are different probability amplitude for the surface and bulk of TI. The expression of collapse and revival has form [44]:

$$t_{col-Floq} = \sqrt{\frac{2Log(10)}{\bar{n}}}\frac{\bar{n}}{\Omega_{Floq}(\bar{n})}, \quad t_{rev-Floq} = \frac{2\pi\bar{n}}{\Omega_{Floq}(\bar{n})}. \tag{11}$$

In Fig. 4**(a)**, it can be seen the collapse time ($t_{col-Floq}$) is decreasing continuously by increasing the number of photons in the cavity. On the other hand, revival time ($t_{rev-Floq}$) has constant nature after some time by increasing the number of photons in the cavity, shown in Fig. 4**(b)**. Form Fig. 4, it can be seen that the collapse and revival time of surface is higher than bulk. It is also justified by the collapse–revival spectra of Floquet frequency, shown in Fig. 3**(a)** and numerical simulation [Table 1]. Therefore, the surface and bulk of TI can be distinguished with help of the collapse–revival phenomenon.

3. Bloch Siegert Shift

When external applied electromagnetic field energy (frequency) is nearly equal to the corresponding particle-hole energy of system i.e. in case of resonance, Rabi oscillation generates. In other words, the Rabi

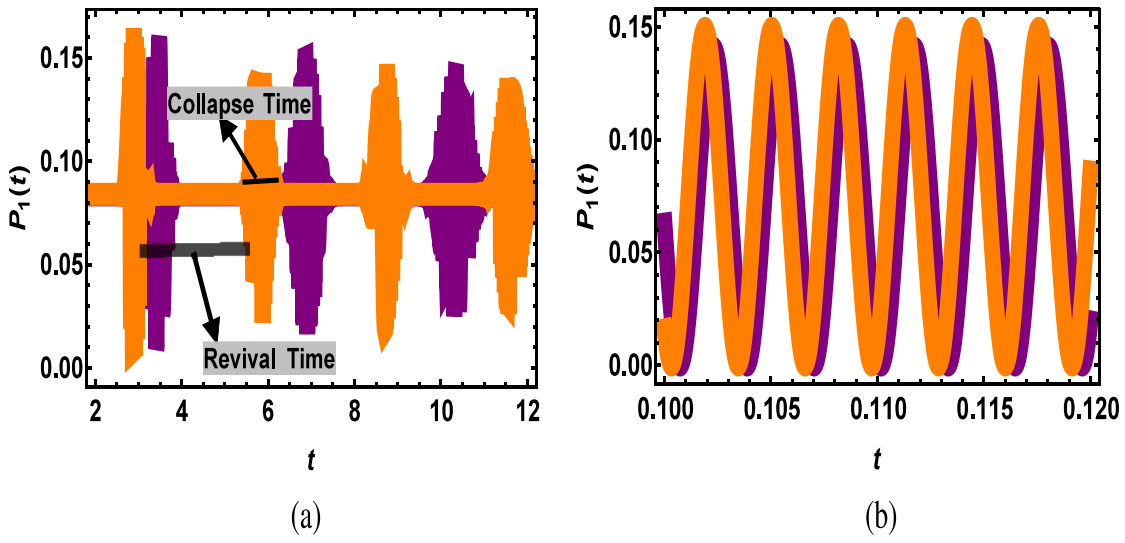

Fig. 3. The plot **(a)** Collapse and revival phenomenon of Floquet oscillations in the bulk (yellow) and surface (purple) of TI. **(b)** If we consider the externally applied field has classical nature, the collapse–revival phenomenon of Floquet oscillations has vanished. The value of mean number of photon $\langle n\rangle = 20$, $|\lambda| = 1$, $B = 1$, $C = -1000$ (bulk), $C = 1000$ (surface), $p = 1$, $\omega_R = 0.1$ and $\omega = 1$, the parameters have dimension of ω^{-1}.

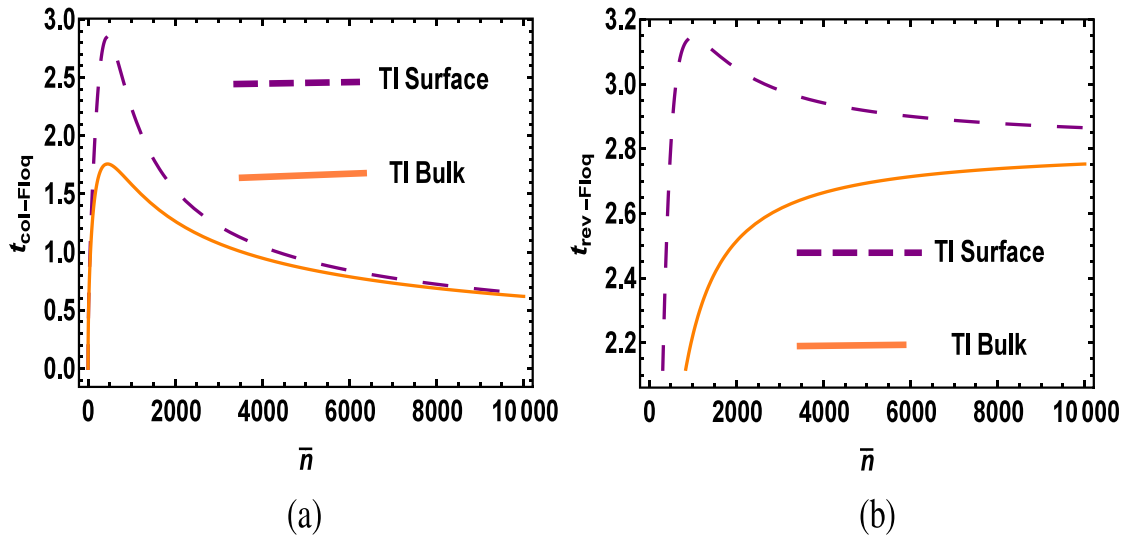

Fig. 4. The plot **(a)** collapse time and **(b)** revival time in bulk and surface of TI. The value of mean number of photon $\langle n\rangle = 20$, $|\lambda| = 1$, $B = 1$, $C = -1000$ (bulk), $C = 1000$ (surface), $p = 1$ and $\omega = 1$. Time has dimension of ω^{-1}.

frequency is the difference of the Floquet–Brillouin zone eigenvalues, also called Rabi splitting [45]. Occupation transfer (Rabi oscillation) and the hybridization of static Floquet sidebands are similar phenomena, the distinction is only seen in the observation method [45]. To describe the Rabi oscillation of the occupation, it is compulsory to refer to the ground state. The ground state belongs to the eigenstate of the static Hamiltonian. When the pump field is present, such solutions are usually not part of the time-dependent Schrödinger equation solutions. Therefore, it is necessary to turn off the field to detect the occupation. On the other hand, the Floquet picture generates the spectrum of the system, when the field is turn-on.

The Rabi oscillation is studied via rotating-wave-approximation (RWA) method. In such approximation, counter-rotating terms (off-resonant transitions) are completely ignored. On increasing field-matter coupling strength, the Jaynes–Cummings model [38] within RWA gives less accuracy. In the case of weak driving field and resonance, RWA is a good approximation but fails in the strong driving regimes [46]. By considering the impact of the counter-rotating terms in RWA (more accuracy), a shift comes in resonance condition of Rabi frequency, called as Bloch–Siegert shift (BSS) [30]. BSS has been already studied in prospective of classical [30,46] and quantized fields [47]. Here, we are studying Rabi oscillation and BSS in TI. It is shown, how behavioral changes come in the Rabi frequency of the surface and Bulk state of TI. By using RWA, the expression of conventional Rabi frequency (Ω_{Rabi}) has found (detail in the supplementary information section(V)) in the TI:

$$\Omega_{\text{Rabi}}(n) = \sqrt{\kappa(n+1)\,|\lambda|^2 + (\omega - 2\epsilon)^2}. \tag{12}$$

Here, $\epsilon = \sqrt{\left(C - Bp^2\right)^2 + p^2v^2}$ and κ is defined as:

$$\kappa = \frac{\left[2C\left(\epsilon - Bp^2\right) + 2C^2 + p^2v^2\right]\left[2B\left(\epsilon + Bp^2 - C\right) + v^2\right]}{v^2\epsilon^2}. \tag{13}$$

After taking counter-rotating terms (rapidly oscillating terms), there are some minute changes in the resonance condition (BSS). In presence

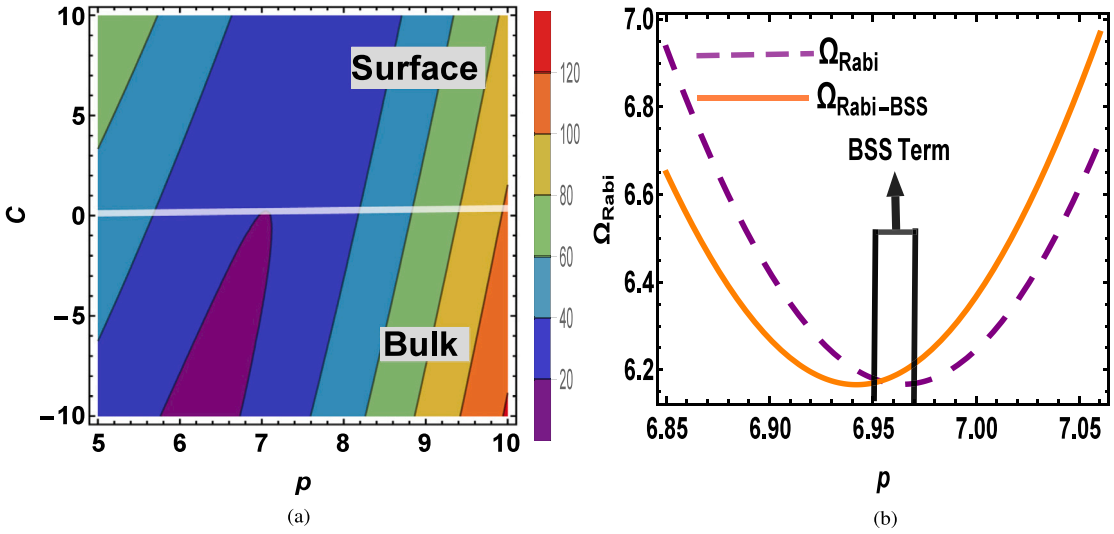

Fig. 5. Contour plot of **(a)** Rabi frequency [Eq. (12)] **(b)** Rabi frequency with BSS [Eq. (14)]. For plotting, we have taken $\lambda = 1$, $n = 99$, $v = 1$, $B = 1$ and $\omega = 100$. Parameters are considered in the unit of λ^{-1}. The surface belongs to the $C > 0$ and bulk belongs to the $C < 0$.

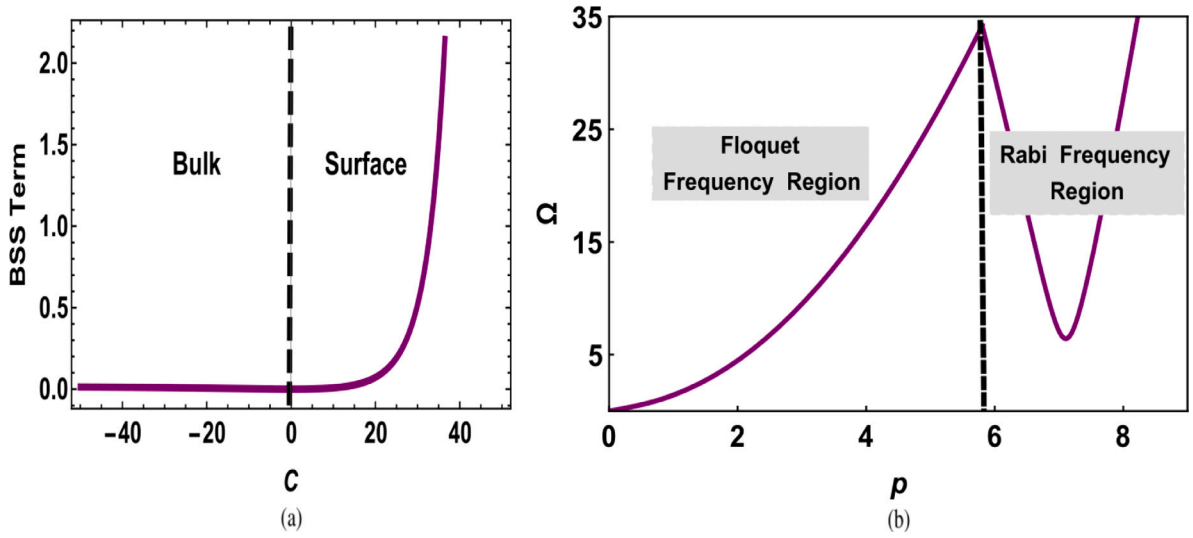

Fig. 6. **(a)** BSS term plot ($p = 7$). **(b)** The cross-over phenomenon between the Floquet and Rabi frequency (Ω_{Floq} or Ω_{Rabi}). For plotting, we have taken $\lambda = 1$, $n = 9$, $B = 1$, $v = 1$, $\omega = 100$ and $C = 1$, parameters are measured in unit of λ^{-1}.

of BSS, the expression of conventional Rabi frequency has form:

$$\Omega_{\text{Rabi-BSS}}(n) = \left[\kappa(n+1)\,|\lambda|^2 - \frac{\gamma^2 (n+1)^2\,|\lambda|^4}{4\epsilon^2} + \left(\omega - 2\epsilon - \frac{\gamma(n+1)\,|\lambda|^2}{2\epsilon} \right)^2 \right]^{\frac{1}{2}}, \tag{14}$$

$$\gamma = \frac{p^2\left[2B^2p^2 - 2B\epsilon + v^2\right] - 2C\epsilon + 2C^2}{4\left[\left(C - Bp^2\right)^2 + p^2v^2\right]}, \tag{15}$$

$$\text{BSS Term} = \frac{\gamma(n+1)\,|\lambda|^2}{2\epsilon}. \tag{16}$$

BSS is a kind of shift in the position of minima. By plotting $\Omega_{\text{Rabi-BSS}}(n)$ and $\Omega_{\text{Rabi}}(n)$, shift in the position of minima can be seen, depicted in Fig. 5**(b)**. The BSS term [Eq. (16)] has dependency on B and C. Therefore, it can be said, the BSS term has a different value in the surface and bulk of TI, shown in Fig. 6**(a)**.

The comparison between behavior of Rabi and Floquet frequency can be seen in Figs. 5**(a)** and 2**(b)**. The Floquet frequency of surface has a very low value in comparison to bulk [Fig. 2**(b)**]. On the other hand, Rabi frequency is showing opposite behavior of Floquet frequency [Fig. 5**(a)**]. So, the Rabi and Floquet frequency can become a tool for detecting the bulk and surface of TI. The Hamiltonian [Eq. (1)] is an expression of TI behavior in low energy (momentum) physics. Fig. 6**(b)** depicts the crossover phenomena between Floquet [Eq. (8)] and Rabi frequency [Eq. (12)] for TI. From Fig. 6**(b)**, it can be seen that Floquet frequency has more dominating nature than Rabi frequency in the low energy (momentum) physics region. Therefore, it can be said, Floquet oscillation is one of the most important phenomena for studying in low energy physics i.e. near the Dirac point.

4. Conclusion

The Floquet and Rabi oscillation have been studied to distinguish the surface and bulk of TI. There is a comparison between the classical and quantum behavior of Floquet oscillation. At the Dirac point in TI, Floquet frequency has zero value on the surface, on the other hand it consists of some threshold value in the bulk. The Floquet collapse–revival spectra show different natures in the surface and bulk state of TI. Rabi frequency shows opposite behavior in comparison to

the Floquet frequency and Bloch–Siegert shift has different values in the surface and bulk of TI. To prove the robustness of the Floquet approximation, a numerical simulation has been performed. It is found that Floquet frequency has dominating nature in comparison to Rabi frequency in low energy physics.

Declaration of competing interest

The authors declare that they have no known competing financial interests or personal relationships that could have appeared to influence the work reported in this paper.

Data availability

No data was used for the research described in the article.

Acknowledgments

We gratefully acknowledge support from the National Research Foundation of Korea, South Korea (2020-M3H4A3081867 and 2022-R1F1A1063060). The computations were carried out using resources from Korea Supercomputing Center (KSC-2022-CRE-0042). Upendra Kumar is highly obliged to the land of Assam (India), the Brahmaputra river, IIT Guwahati, Kamakhya temple, and Prof. Girish S. Setlur, who has given him the motivation to work in core physics research.

Appendix A. Supplementary data

Supplementary material related to this article can be found online at https://doi.org/10.1016/j.physe.2022.115496.

References

[1] C.L. Kane, E.J. Mele, Z_2 topological order and the quantum spin hall effect, Phys. Rev. Lett. 95 (2005) 146802.
[2] C. Noguera, Polar oxide surfaces, J. Phys. Condens. Matter. 12 (2000) R367.
[3] A. Burkov, L. Balents, Weyl semimetal in a topological insulator multilayer, Phys. Rev. Lett. 107 (2011) 127205.
[4] G. Floquet, Sur les équations différentielles linéaires à coefficients périodiques, Ann. Sci. De L'école Normale Supérieure 12 (1883) 47–88.
[5] A. Eckardt, E. Anisimovas, High-frequency approximation for periodically driven quantum systems from a floquet-space perspective, New J. Phys. 17 (2015) 093039.
[6] R. Merlin, Rabi oscillations, floquet states, Fermi's golden rule, and all that: Insights from an exactly solvable two-level model, Amer. J. Phys. 89 (2021) 26.
[7] H.L. Calvo, H.M. Pastawski, S. Roche, L.E.F. Torres, Tuning laser-induced band gaps in graphene, Appl. Phys. Lett. 98 (2011) 232103.
[8] R. Wang, B. Wang, R. Shen, L. Sheng, D. Xing, Floquet Weyl semimetal induced by off-resonant light, Europhys. Lett. 105 (2014) 17004.
[9] T. Nakai, C.A. McDowell, An analysis of NMR spinning sidebands of homonuclear two-spin systems using floquet theory, Mol. Phys. 77 (1992) 569.
[10] E.S. Mananga, T. Charpentier, Introduction of the floquet-magnus expansion in solid-state nuclear magnetic resonance spectroscopy, J. Chem. Phys. 135 (2011) 044109.
[11] J. Cayssol, B. Dóra, F. Simon, R. Moessner, Floquet topological insulators, Phys. Status Solidi RRL 7 (2013) 101.
[12] T. Kitagawa, E. Berg, M. Rudner, E. Demler, Topological characterization of periodically driven quantum systems, Phys. Rev. B 82 (2010) 235114.
[13] Y. Wang, H. Steinberg, P. Jarillo-Herrero, N. Gedik, Observation of floquet-bloch states on the surface of a topological insulator, Science 342 (2013) 453.
[14] F. Mahmood, C.-K. Chan, Z. Alpichshev, D. Gardner, Y. Lee, P.A. Lee, N. Gedik, Selective scattering between Floquet–Bloch and Volkov states in a topological insulator, Nat. Phys. 12 (2016) 306.
[15] B.M. Fregoso, Y. Wang, N. Gedik, V. Galitski, Driven electronic states at the surface of a topological insulator, Phys. Rev. B 88 (2013) 155129.
[16] H.L. Calvo, L.F. Torres, P.M. Perez-Piskunow, C.A. Balseiro, G. Usaj, Floquet interface states in illuminated three-dimensional topological insulators, Phys. Rev. B 91 (2015) 241404.
[17] B. Dóra, J. Cayssol, F. Simon, R. Moessner, Optically engineering the topological properties of a spin hall insulator, Phys. Rev. Lett. 108 (2012) 056602.
[18] N.H. Lindner, G. Refael, V. Galitski, Floquet topological insulator in semiconductor quantum wells, Nat. Phys. 7 (2011) (2011) 490.
[19] D.E. Liu, A. Levchenko, H.U. Baranger, Floquet Majorana fermions for topological qubits in superconducting devices and cold-atom systems, Phys. Rev. Lett. 111 (2013) 047002.
[20] A. Giorgio, A.G. Perri, M.N. Armenise, Design of guided-wave photonic bandgap devices by using the bloch-floquet theory, Opt. Eng. 42 (2003) 1100.
[21] A. Russomanno, S. Pugnetti, V. Brosco, R. Fazio, Floquet theory of cooper pair pumping, Phys. Rev. B 83 (2011) 214508.
[22] T. Oka, S. Kitamura, Floquet engineering of quantum materials, Annu. Rev. Condens. Matter Phys. 10 (2019) 387.
[23] R. Silva, I.V. Blinov, A.N. Rubtsov, O. Smirnova, M. Ivanov, High-harmonic spectroscopy of ultrafast many-body dynamics in strongly correlated systems, Nat. Photon. 12 (2018) 266.
[24] Y. Murakami, M. Eckstein, P. Werner, High-harmonic generation in mott insulators, Phys. Rev. Lett. 121 (2018) 057405.
[25] I. Martin, G. Refael, B. Halperin, Topological frequency conversion in strongly driven quantum systems, Phys. Rev. X 7 (2017) 041008.
[26] C. Weitenberg, J. Simonet, Tailoring quantum gases by floquet engineering, Nat. Phys. 17 (2021) 1342.
[27] I.I. Rabi, Space quantization in a gyrating magnetic field, Phys. Rev. 51 (1937) 652.
[28] P. Forn-Díaz, J. Lisenfeld, D. Marcos, J.J. Garcia-Ripoll, E. Solano, C. Harmans, J. Mooij, Observation of the bloch-siegert shift in a qubit-oscillator system in the ultrastrong coupling regime, Phys. Rev. Lett. 105 (2010) 237001.
[29] H. Haug, S.W. Koch, Quantum Theory of the Optical and Electronic Properties of Semiconductors, fivth ed., World Scientific Publishing Company, 2009.
[30] F. Bloch, A. Siegert, Magnetic resonance for nonrotating fields, Phys. Rev. 57 (1940) 522.
[31] L.V. Vela-Arevalo, R.F. Fox, Coherent states of the driven rydberg atom: Quantum–classical correspondence of periodically driven systems, Phys. Rev. A 71 (2005) 063403.
[32] H.F. Talbot, LXXVI. Facts relating to optical science. No. IV, Phil. Mag. 9 (1836) 401.
[33] A. Bakman, H. Veksler, S. Fishman, Collapse and revival for a slightly anharmonic hamiltonian, Phys. Lett. A 381 (2017) 2298.
[34] J.A. Yeazell, C. Stroud Jr., Observation of fractional revivals in the evolution of a Rydberg atomic wave packet, Phys. Rev. A 43 (1991) 5153.
[35] J.H. Eberly, N. Narozhny, J. Sanchez-Mondragon, Periodic spontaneous collapse and revival in a simple quantum model, Phys. Rev. Lett. 44 (1980) 1323.
[36] A. Iurov, L. Zhemchuzhna, G. Gumbs, D. Huang, Exploring interacting floquet states in black phosphorus: Anisotropy and bandgap laser tuning, J. Appl. Phys. 122 (2017) 124301.
[37] B. Dey, T.K. Ghosh, Photoinduced valley and electron–hole symmetry breaking in α-t 3 lattice: The role of a variable berry phase, Phys. Rev. B 98 (2018) 075422.
[38] E.T. Jaynes, F.W. Cummings, Comparison of quantum and semiclassical radiation theories with application to the beam maser, Proc. IEEE 51 (1963) 89.
[39] F.D.M. Haldane, Model for a quantum hall effect without Landau levels: Condensed-matter realization of the parity anomaly, Phys. Rev. Lett. 61 (1988) 2015.
[40] M.Z. Hasan, C.L. Kane, Colloquium: Topological insulators, Rev. Modern Phys. 82 (2010) 3045.
[41] S.-Q. Shen, W.-Y. Shan, H.-Z. Lu, Topological insulator and the Dirac equation, Spin 1 (2011) 33.
[42] W.R. Inc, Mathematica, Version 11.1, champaign, IL, 2017.
[43] Z. Ficek, M.R. Wahiddin, Quantum Optics for Beginners, CRC Press, 2014.
[44] Enamullah, V. Kumar, U. Kumar, G.S. Setlur, Quantum rabi oscillations in graphene, J. Opt. Soc. Amer. B 31 (2014) 484.
[45] U. De Giovannini, H. Hübener, Floquet analysis of excitations in materials, J. Phys.: Mater. 3 (2019) 012001.
[46] J.H. Shirley, Solution of the Schrödinger equation with a Hamiltonian periodic in time, Phys. Rev. 138 (1965) B979.
[47] P. Hannaford, D.T. Pegg, G.W. Series, Analytical expressions for the bloch-siegert shift, J. Phys. B 6 (1973) L222.